

# Estimating inter-event time distributions from finite observation periods in communication networks

Mikko Kivelä<sup>1</sup> and Mason A. Porter<sup>1,2</sup>

<sup>1</sup>*Oxford Centre for Industrial and Applied Mathematics,  
Mathematical Institute, University of Oxford, Oxford OX2 6GG, UK*  
<sup>2</sup>*CABDyN Complexity Centre, University of Oxford, Oxford OX1 1HP, UK*  
(Dated: July 6, 2022)

A diverse variety of processes — including recurrent disease episodes, neuron firing, and communication patterns among humans — can be described using inter-event time (IET) distributions. Many such processes are ongoing, although event sequences are only available during a finite observation window. Because the observation time window is more likely to begin or end during long IETs than during short ones, the analysis of such data is susceptible to a bias induced by the finite observation period. In this paper, we illustrate how this length bias is born and how it can be corrected. To do this, we model event sequences using stationary renewal processes, and we formulate simple heuristics for determining the severity of the bias. To illustrate our results, we focus on the example of empirical communication networks, which are temporal networks that are constructed from communication events. The IET distributions of such systems guide efforts to build models of human behavior, and the variance of IETs is very important for estimating the spreading rate of information in networks of temporal interactions. It is thus crucial to have good estimates for the statistics of IET tails. We analyze several well-known data sets from the literature, and we find that the vast majority of event sequences of these data sets are susceptible to finite window-size effects. We demonstrate that the resulting bias can lead to systematic underestimates of the variance in the IET distributions and that correcting for the bias can lead to *qualitatively* different results for the tails of the IET distributions — and this is especially true for IETs with heavy-tails, which are often of interest.

The newfound wealth of large data sets in the modern era of “Big Data” necessitates statistical analyses of such data. This has been especially prevalent in the study of human behavior, and the digital footprints left behind by electronic activities have provided a deluge of data. One of the most important problems in the study of human dynamics, which benefits directly from such data, is to quantify temporal activity patterns in human behavior. For example, this problem has been approached via the characterization of time sequences of human activities [1–7] and the analysis of “temporal networks” [8] (i.e., networks that change in time). *Inter-event times* (IETs) give the times between each pair of events (e.g., sending an e-mail, making a phone call, or doing any other activity), and the way they are distributed has received intense scrutiny because they can be used to characterize temporal processes. IET distributions have a long history — for example, they are important in fields such as medicine and engineering [9–11] — and they have become particularly important for the study of large temporal data sets. Recently, they have been used to guide the modeling of human-activity dynamics [2–4, 6, 12, 13], and they are also important for temporal networks, where they can have a large effect on processes that act on top of such networks [8, 14]. For example, spreading processes are sensitive to the bursty nature of the time sequences of contacts, which tend to be characterized by heavy-tailed inter-contact time distributions [15–19].

Electronic records often have a huge number of data points. Such data often includes many subjects, but it may or may not also include a similar wealth of longi-

tudinal points. For example, there exist data sets with thousands or even millions of people but with observation periods that only last a few months [1, 5, 17]. Moreover, even when the observation period is long, a given individual might rarely be active during that time. This is the case, for example, in recent studies of e-mail communication [1–3, 6, 20], mobile phone calling [17, 18], website usage [4], and donations to charities [21]. Data sets that describe human activity in which the observation windows are comparable in scale to the IETs are vulnerable to finite-size biases, because the time interval between events is more likely to be truncated artificially by the boundaries of a time window when it is longer, then. This can arise due to short observation windows and/or sparse records of activity. This effect will bias the tails of the observed IET distributions, which is a very serious issue, as the properties of distribution tails are often among the most important empirical features that one needs to consider [8] and models of human dynamics have been validated or refuted based on their predictions of the shape of the IET distributions [2, 3, 6, 7, 12, 13]. Furthermore, the variance of the IET distributions can have a large effect on the speed of spreading processes [15–18], and it has been used to classify the processes that produce them [20].

Several approaches have been used to deal with the bias introduced by a finite temporal-window size. In particular, it is common to disregard all of the boundary effects and use the observed IETs [4, 5, 20]. Such biases are sometimes acknowledged: for example, the exponential tail of the IET distribution is sometimes construed as

a finite-size effect [7]. One can ameliorate the bias somewhat by introducing temporal periodic boundary conditions [17, 18], but such a solution still does not give an unbiased estimator for an IET distribution. Another approach to dealing with a finite observation period is to correct the probability of observing an IET value by dividing it by the probability that an IET of that length is not truncated by the observation window [22]. As we will discuss later, for stationary renewal processes, the latter probability always declines linearly when the observed IET length grows. This linear correction has also been observed in empirical data by resampling using different observation window sizes [15].

The error in an observed IET distribution is very small if the tail of the IET distribution is sufficiently short relative to the length of the time window. This is usually the case if one uses event sequences with a large number of events. Unfortunately, in practice this tends to entail that one can use only a small subset of available data. For example, some studies on temporal communication patterns that were based on data sets of thousands of people only used subsets of the most active people that ranged from a single person to about 10% of the data [2, 6, 7]. This approach discards valuable data and biases the analysis towards the behavior of very active individuals.

The problem of inferring an IET distribution from a finite observation period arises in a diverse set of fields — such as engineering and medicine, where the problem has been studied using renewal processes [9] and other models for recurrent events [10, 11]. For example, consider a factory that contains machines that break after some random time and after which they need to be replaced. In reliability analysis, one might want to design an experiment in which one records the exact times when a machine breaks for some time interval to attempt to infer the distribution of the times that the machine can go without replacing. In mathematical terms, one can construe this scenario as exactly the same problem as recording time stamps of e-mails sent by an individual and inferring the distribution of times between e-mails. Due to the generic nature of the problem, several statistical tools have been developed for estimating the IET distributions for renewal processes [23–29]. Similar problems have also been encountered when estimating inter-spike intervals of firing neurons [30].

In this paper, we concentrate on stationary renewal processes because they are minimal models for producing event sequences with arbitrary IET distributions. However, real world processes are often more complicated than stationary renewal processes. For example, communication patterns and many natural phenomena, such as earthquakes or neuronal spike trains, are created using processes that have memory [20, 31]. One should also be careful when assuming the stationarity of the process. Other processes, such as inhomogeneous Poisson processes and processes in which cascades of activity can be triggered by prior events, also yield tractable models for human dynamics [6, 32, 33].

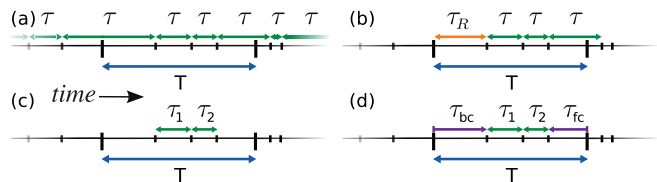


FIG. 1. (a) A stationary renewal process generates an infinite sequence of events. We place a time window of length  $T$  in an arbitrary place on the timeline. (b) We consider only the events that lie inside of the time window. The time from the start of the time window to the first event is the *residual waiting time*  $\tau_R$ , and one can derive its distribution from  $p(\tau)$  [9]. (c) The *observed inter-event times* are the IETs that lie completely inside of the time window. (d) The *censored IETs* are the ones that are cut by the time window. An IET that is cut by the end of the time window is said to be *forward censored*. An IET that is truncated must be longer than the forward censoring time  $\tau_{fc} \leq \tau_3$ . Similarly, an IET that is cut by the start of the time window is said to be *backward censored*, and the backward censoring time  $\tau_{bc}$  satisfies  $\tau_{bc} \leq \tau_0$ . [34]

*IET distributions from stationary renewal processes.* We concentrate on a model for producing  $N$  event sequences observed in a finite time window of length  $T$ . The model can have an arbitrary IET distribution  $p(\tau)$ , and we assume that each IET is independent of all of the prior ones. We also assume that the process that produces the events is in a stationary state at the starting time of the observation window and that the starting time is selected independently of the state of process. These assumptions amount to assuming that we have a stationary renewal process. See Fig. 1a,b for an illustration.

*Estimation of inter-event time distributions.* We seek to estimate the original IET distribution  $p(\tau)$  when we are given only the time stamps of the events inside of the observation window. A naive method would be to use the distribution  $p'(\tau)$  for observed IETs to estimate the original distribution (see Fig. 1c). Unfortunately, the observed IETs and the real IETs do not follow the same distribution.

In Fig. 2, we illustrate the difference between  $p(\tau)$  and  $p'(\tau)$  for exponential and power-law IET distributions. This difference grows linearly when the IET length  $\tau$  approaches the window size  $T$ , and  $p'(\tau) = 0$  for  $\tau > T$ . This occurs because a longer IET makes it more likely that the observation window will either start or end between the two events that correspond to that IET. Observed IETs are always distributed so that there is a linear cutoff at the end of the time window  $T$ . In other words,

$$p'(\tau) \propto (T - \tau)p(\tau) \quad (1)$$

when the number of event sequences  $N \rightarrow \infty$  [26]. In the worst case, this bias can lead to qualitatively incorrect conclusions about the shape of the tail of an IET distribution. It is therefore important to correct for this bias.

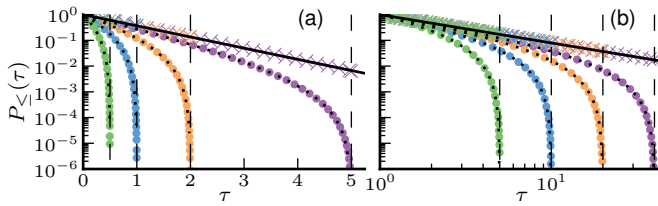


FIG. 2. We plot cumulative IET distributions  $P_{\le}(\tau)$  for  $N = 10^5$  event sequences that we simulate from a stationary renewal process for which (a)  $p(\tau) \propto e^{-\tau}$  and (b)  $p(\tau) \propto \tau^{-2.1}$ . We consider window sizes  $T$  (which we mark with dashed vertical lines) of (a) 0.5, 1, 2, and 5 and (b) 5, 10, 20, and 40. The dots mark the observed IET distribution, and the crosses mark the estimates of the original IET distribution using the Kaplan–Meier (KM) estimator. The solid black line is the theoretical  $p(\tau)$  distribution, and the dotted curves are the theoretical distributions for IETs [ $p'(\tau) \propto (T - \tau)p(\tau)$ ] that lie completely inside of each time window. A nonparametric maximum likelihood estimation (NPMLE) estimator [26] gives qualitatively similar results.

There exist both parametric [29] and nonparametric [11, 23–28] estimators for the original IET distribution  $p(\tau)$ . A straightforward nonparametric way to estimate IETs is to use the Kaplan–Meier (KM) estimator [35] by considering the IETs inside of the time window as uncensored observations and the IETs that are truncated by the end of the time window as censored observations [24, 36]. Additionally, because the process of generating event sequences is symmetric in time, we can increase the accuracy of our estimate by repeating this estimation process backwards in time [24]. That is, we include each uncensored IET twice, and we include the censored IETs at the boundaries of the time window only once [37]. One can estimate the variance of the KM estimator using Greenwood’s formula [35, 38], which has to be modified slightly to take into account double-counting of the uncensored IETs [24]. See Fig. 1d for a schematic and Fig. 2 for an example how the KM estimator corrects the bias introduced by the finite observation window for simulated data. See Section B of the Supplementary Materials (SM) for more information.

The KM estimator is simple to calculate, but it discards some of the information about the process of how an IET is generated. Vardi [23] defined a nonparametric maximum likelihood estimation (NPMLE) method for data produced with a stationary renewal process. Reference [26] later generalized Vardi’s method for continuous-time situations as well as for situations in which there are also empty event sequences. Note, however, that methods based on the KM estimator and Vardi’s NPMLE can yield estimates that are very close to each other even though the KM estimator is more computationally efficient than Vardi’s NPMLE estimator [24]. One can also use a reduced-sample estimator, which ignores data points close to the boundaries of the observation window, but Pawlas et al. [30] observed for several different generative models of event sequences that

it gives less accurate estimates than a method based on the KM estimator.

*When does one need to worry about finite window-size effects?* The bias introduced by using the observed IET distribution as an estimate for an underlying IET distribution for a given process can be very small even if data is produced by sampling from a renewal process using a finite time window. This is the case if the time-window length is sufficiently long in comparison to the underlying IET distribution. In this case, one does not need to worry about finite-size effects or make any corrections to account for them. We will give some guidelines for determining when this happy situation holds.

As we discussed earlier, the bias in an IET distribution grows linearly with IET length. It is thus useful to compare the bias in the smallest observed IET to the bias in the largest observed IET, as this ratio gives an estimate for the largest error in the distribution. If the smallest observed IET is 0, then Eq. (1) implies that

$$\frac{p'(\tau)}{p'(0)} = \left(1 - \frac{\tau}{T}\right) \frac{p(\tau)}{p(0)}. \quad (2)$$

Equation (2) can be used as a rule of thumb for assessing if a finite time window distorts an observed IET distribution. For example, if the largest data point (i.e., the rightmost point in an observed IET distribution) is more than 100 times smaller than the length of the observation window, then the error that results using the observed IETs for estimating the real IET distribution is less than 1% for IET values smaller than the maximum observed IET value.

Equation (2) gives an estimate for the relative probabilities of observed IETs, but it does not indicate anything about the distribution’s tail, which is not observed. This can be an issue if one has very small amounts of data or if one wants to calculate summary statistics of an IET distribution that are very sensitive to the properties of tail (e.g., moments of an IET distribution, measures of event burstiness, and so on). The moments  $\mu'_m$  of an observed IET distribution are lower than the moments  $\mu_m$  of the real IET distribution. However, if we have an estimate  $p^{\text{est}}(\tau)$  for the real IET distribution  $p(\tau)$  for  $\tau \leq T$ , then we can estimate the moments using

$$\mu_m^{\text{est}} = \int_0^T \tau^m p^{\text{est}}(\tau) d\tau + T^m P_{\le}^{\text{est}}(T), \quad (3)$$

where  $P_{\le}$  is the cumulative distribution of the IET. Assuming that the estimate for IET distribution is perfect (i.e.,  $p^{\text{est}}(\tau) = p(\tau)$  when  $\tau \leq T$ ), we obtain a sharper lower bound for the moments using  $\mu_m^{\text{est}}$  than using  $\mu'_m$ . That is,  $\mu'_m \leq \mu_m^{\text{est}} \leq \mu_m$ . We illustrate this issue later using empirical data, and we discuss the estimation of moments further in the SM.

*Analysis of empirical data.* We now use the methods that we described above to reanalyze several public data sets from the literature. For each of these data sets, we concentrate on the temporal sequences of messages that are sent by individuals.

The Eckmann et al. e-mail data set [1] contains time stamps of about  $3 \times 10^5$  e-mails between 3188 people during 83 days. This data set has been examined by several authors, and the shape of the IET distributions of individuals with high e-mailing frequencies has received particularly close scrutiny (and has attracted controversy) [2, 6, 39, 40]. The pussokram.com (POK) data [4, 22] is a communication record of an online community with about  $3 \times 10^4$  people who sent  $5 \times 10^5$  messages during the entire 492-day lifetime of the site. It is not reasonable to construe message sequences in this data set as having been produced by a stationary renewal process because the data were recorded started from the birth of the POK website. However, it is still reasonable to consider the data as being forward censored (see Fig. 1). Reference [4] plotted the distribution of all IETs as well as distributions grouped according to the number of sent messages. These plots contain noticeable dips at the end of the IET distributions, but it was not clear if this feature arises because of intrinsic human behavior or is instead due to the finite length of the data. A third data set that we examine was introduced by Wu et al. [7], who studied IETs of short messages sent within three different companies during one month. We present our reanalysis of data from company 1, which includes about  $5 \times 10^5$  messages sent by about  $4 \times 10^4$  people. The results for the two other companies are similar. To get good statistics, Wu et al. concentrated on communication patterns between the few pairs of users who sent very large numbers of messages. For each data set, we consider the message-sending times of each person as a single event sequence.

Each of the data sets includes a large number of IETs that are sufficiently close to the time-window length to affect the observed IET distribution. We illustrate this fact in panels (a)–(c) of Fig. 3. For each data set, we show both the observed IET distribution and the KM estimate of the IET distribution. It is clear that the shape of the tail of the observed IET distributions is qualitatively different from that of the KM estimate of the IET distribution.

In Table I, we compare some summary statistics of the KM estimate of the IET distributions and the observed IET distributions to gain better understanding of the magnitude of the difference between the two. The first two moments and residual waiting times calculated from the IET distribution given by the KM estimator are often more than 100% larger than ones calculated from the observe IET distribution. These differences can have a huge impact on processes acting on top of such temporal networks, and it is clear that the bias introduced by a finite observation-window size can be a major problem in these data sets. For example, the mean residual waiting time  $\tau_R$  — which is vastly smaller when calculated using the observed IET distributions than when calculated using the IET distributions obtained with the KM estimator — is related to the speed of spreading in networks [15–19] because it is the expected time that one

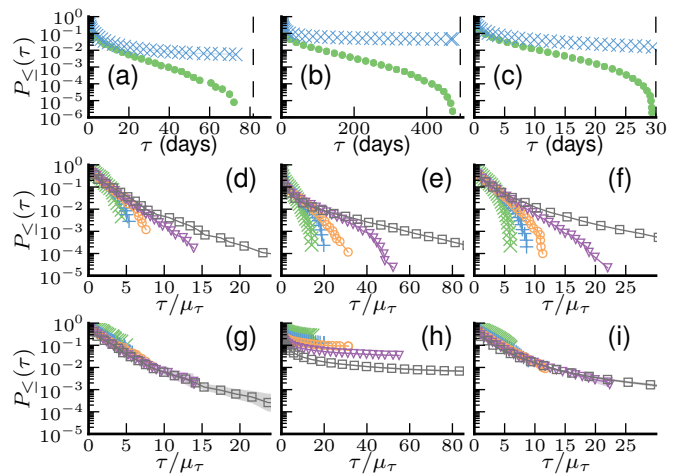


FIG. 3. Results for the empirical data sets. Panels (a)–(c) show IET distributions for all node activation sequences. The dots mark the observed IET distributions, and the crosses mark the estimates of the original IET distributions using the KM estimator. Panels (d)–(f) show cumulative distributions of observed IETs, and panels (g)–(i) show KM estimates for the cumulative IET distributions. The shaded regions are the 95% confidence intervals [24]. We bin the event sequences according to the number of events in them ( $\times$ :  $n = 2$ ,  $+$ :  $n = 5$ ,  $\circ$ :  $n \in [7, 8]$ ,  $\nabla$ :  $n \in [13, 24]$ ,  $\square$ :  $n \in [50, 149]$ ; we skip every other bin to make the figure easier to read), and we normalize them according to the bin’s mean IET  $\mu_\tau$ . The data sets are (a, d, g) Eckmann et al. e-mail data [1], (b, e, h) POK messages [4], and (c, f, i) Wu et al. short message data [7].

Data	$\mu'_1$	$\mu_1^{\text{km}}$	$\sqrt{\mu'_2}$	$\sqrt{\mu_2^{\text{km}}}$	$\mu'_1(\tau_R)$	$\mu_1^{\text{km}}(\tau_R)$	$\tau_{f,c,bc}$
E-mail	0.908	1.51	3.20	6.88	5.62	15.6	17.5
POK	5.13	28.4	23.1	106	51.9	198	240
Short message	0.633	1.40	2.11	4.89	3.53	8.53	8.73

TABLE I. The first two moments of the IETs calculated from the observed IET distribution and using Eq. (3) for the IET distribution produced by the KM estimator, estimates of the residual waiting times using the formula  $\mu_1(\tau_R) = \frac{1}{2} \frac{\mu_2}{\mu_1}$  [18], and the mean of both forward and backward censoring times  $\tau_{f,c,bc}$  for all data sets. Note that data produced by a stationary renewal process has forward-censoring and backward-censoring times that are distributed as the residual waiting times for values that are smaller than the window size  $T$ .

has to wait for the next event after a node is infected at a time chosen uniformly at random.

In studies of empirical data it is often supposed that each event sequence is produced by an IET distribution with the same characteristic shape  $f$  but with a different mean value  $\tau_0$  [4, 5, 17, 20, 41, 42]. The IET distribution for a sequence with mean  $\tau_0$  is  $p(\tau|\tau_0) = \frac{1}{\tau_0} f(\tau/\tau_0)$ . See Section D in SM for more information. In panels (d)–(i) of Fig. 3, we plot the IET distributions (for each data set) in which we group event sequence with similar numbers of events. We include event sequences that have fewer than 150 events because sequences with few

events are the most susceptible to finite-size effects. Sequences with at most 149 events encompass 90%–99% of all sequences (depending on the data set). We observe that normalized IET distributions for event sequences with few events decrease much faster than the IET distributions for sequences with many events. This result is as expected, and it results from the bias introduced by the finite observation window. There is a very good collapse of the tails of the KM estimates of the normalized IET distributions for the e-mail communication and short-message communication data. This is remarkable, given that collapse is not expected to be perfect even for data that perfectly follows the characteristic distribution model (see Section D in SM). The difference between the IET distributions of the POK data and the two other data sets is possibly due to users who leave the service permanently. This process would lead to the last IET being infinitely long, which would manifest as the tail of the cumulative distribution approaching a value that corresponds to the fraction of people in each group who have left the service. If the probability of leaving the service is lower for people that have sent a large number of messages, then one would then expect to observe the tails of the cumulative distributions of groups with large numbers of messages to approach lower values than the groups with small numbers of messages.

*Conclusions and Discussion.* We investigated the effects that a finite observation window can have on observed inter-event times (IETs). For a stationary renewal process, we illustrated that the finite time window introduces a linear cutoff to the observed IET distribution at the end of the time window. We also showed how to correct this bias using nonparametric estimators, such as a KM estimator or an NPMLE, for a stationary renewal process even if the number of events is small by grouping the event sequences. We then used these methods to reanalyze three data sets of human communication, and we found that using the observed IET distributions without correcting for the finite-size bias can seriously distort the shape and key summary statistics of the IET distributions.

Event sequences for human behavior are rather heterogeneous: they contain widely disparate numbers of

events. However, many authors have argued that it is possible to represent such sequences using a characteristic function that is independent of the underlying rate of events [5, 17, 20, 41, 42]. Methods for testing whether an IET distribution has some specific shape conditional on the underlying rate of events are also susceptible to finite-size effects, and parametric analogs of the methods that we have employed should be applied in such situations [29]. Moreover, there is an additional bias if one infers the underlying rate from the observed number of events, and it is important to develop statistical methods that are able to assume an underlying model for a characteristic IET distribution.

The need for the wide dissemination and use of correction methods like KM estimators or NPMLEs for IET distributions is underscored by the rapidly growing analysis of temporal data streams. Nonparametric methods for correcting for biases introduced by a finite observation window have existed for several decades [23, 24, 26]. Surprisingly, such methods (to our knowledge) do not seem to have been used when analyzing human communication patterns, although there have been some ad-hoc attempts to directly correct for the linear bias [15, 22]. Additionally, although we have focused on human communication patterns, the problem of correcting for these finite-size effects is a general one, and similar methods have been reinvented in multiple fields. For example, the KM estimator was used for window-censored data in the 1980s [24], and its use for such data was independently reinvented many years later in the context of estimating the interspike intervals of neurons [30]. Appropriately taking into account finite-size effects makes it possible to obtain accurate estimates for the tail of an IET distribution and to optimally exploit data that consists of a large number of event sequences with only a small number of events (as opposed to high-frequency event sequences, which are largely free of such significant finite-size effects).

*Acknowledgements.* Both authors were supported by the European Commission FET-Proactive project PLEXMATH (Grant No. 317614). We thank Andrea Bertozzi, Carlos Gershenson, and Jari Saramäki for helpful comments; and we thank Jean-Pierre Eckmann for providing us with the e-mail data set.

- 
- [1] J.-P. Eckmann, E. Moses, and D. Sergi, *Proc. Natl. Acad. Sci. U.S.A.* **101**, 14333 (2004).
  - [2] A. L. Barabási, *Nature* **435**, 207 (2005).
  - [3] A. Vázquez, J. G. Oliveira, Z. Dezsö, K.-I. Goh, I. Kondor, and A.-L. Barabási, *Phys. Rev. E* **73**, 036127 (2006).
  - [4] D. Rybski, S. V. Buldyrev, S. Havlin, F. Liljeros, and H. A. Makse, *Sci. Reps.* **2**, 560 (2012).
  - [5] J. Candia, M. C. González, P. Wang, T. Schoenharl, G. Madey, and A.-L. Barabási, *J. Phys. A: Math. Theor.* **41**, 224015 (2008).
  - [6] R. D. Malmgren, D. B. Stouffer, A. E. Motter, and L. A. Amaral, *Proc. Natl. Acad. Sci. U.S.A.* **105**, 18153 (2008).
  - [7] Y. Wu, C. Zhou, J. Xiao, J. Kurths, and H. J. Schellnhuber, *Proc. Natl. Acad. Sci. U.S.A.* **107**, 18803 (2010).
  - [8] P. Holme and J. Saramäki, *Phys. Reps.* **519**, 97 (2012).
  - [9] W. Feller, *An Introduction to Probability Theory and Its Applications*, Vol. 2 (Wiley, 1971).
  - [10] W. B. Nelson, *Recurrent Events Data Analysis for Product Repairs, Disease Recurrences, and Other Applications*, Vol. 10 (SIAM, 2003).
  - [11] R. J. Cook and J. F. Lawless, *The Statistical Analysis of Recurrent Events* (Springer, 2007).

- [12] B. Min, K.-I. Goh, and I.-M. Kim, *Phys. Rev. E* **79**, 056110 (2009).
- [13] J. Oliveira and A. Vazquez, *Physica A* **388**, 187 (2009).
- [14] M. A. Porter and J. P. Gleeson, “Dynamical systems on networks: A tutorial,” (2014), arXiv:1403.7663 [nlin.AO].
- [15] A. Vazquez, B. Rácz, A. Lukács, and A.-L. Barabási, *Phys. Rev. Lett.* **98**, 158702 (2007).
- [16] G. Miritello, E. Moro, and R. Lara, *Phys. Rev. E* **83**, 045102 (2011).
- [17] M. Karsai, M. Kivelä, R. K. Pan, K. Kaski, J. Kertész, A.-L. Barabási, and J. Saramäki, *Phys. Rev. E* **83**, 025102 (2011).
- [18] M. Kivelä, R. K. Pan, K. Kaski, J. Kertész, J. Saramäki, and M. Karsai, *J. Stat. Mech.* **2012**, P03005 (2012).
- [19] H.-H. Jo, J. I. Perotti, K. Kaski, and J. Kertész, *Phys. Rev. X* **4**, 011041 (2014).
- [20] K.-I. Goh and A.-L. Barabási, *Europhys. Lett.* **81**, 48002 (2008).
- [21] A. Wipprecht, M.Sc. thesis, Mathematical Modelling and Scientific Computation, University of Oxford (2011), available at [http://people.maths.ox.ac.uk/porterm/research/annika\\_Dissertation\\_final.pdf](http://people.maths.ox.ac.uk/porterm/research/annika_Dissertation_final.pdf).
- [22] P. Holme, *Europhys. Lett.* **64**, 427 (2003).
- [23] Y. Vardi, *Ann. Stat.* **10**, 772 (1982).
- [24] L. Denby and Y. Vardi, *Technometrics* **27**, 361 (1985).
- [25] S. McClean and C. Devine, *Biometrika* **82**, 791 (1995).
- [26] G. Soon and M. Woodroffe, *J. Stat. Plan. Inference* **53**, 171 (1996).
- [27] E. A. Peña, R. L. Strawderman, and M. Hollander, *JASA* **96**, 1299 (2001).
- [28] R. D. Gill and N. Keiding, *Lifetime Data Anal.* **16**, 571 (2010).
- [29] Y. Zhu, E. Yashchin, and J. Hosking, *Technometrics* **56**, 55 (2014).
- [30] Z. Pawlas and P. Lansky, *Phys. Rev. E* **83**, 011910 (2011).
- [31] M. Karsai, K. Kaski, A.-L. Barabási, and J. Kertész, *Sci. Reps.* **2**, 397 (2011).
- [32] R. D. Malmgren, D. B. Stouffer, A. S. Campanharo, and L. A. N. Amaral, *Science* **325**, 1696 (2009).
- [33] J. R. Zipkin, F. P. Schoenberg, K. Coronges, and A. L. Bertozzi, Unpublished manuscript (2014).
- [34] Note that we don’t use the terminology “censored on the right” and “censored on the left” because we want to avoid confusion with the terms “right censored” and “left censored”.
- [35] E. L. Kaplan and P. Meier, *JASA* **53**, 457 (1958).
- [36] R. Gill, *Ann. Stat.* **9**, 853 (1981).
- [37] We call this estimator “the KM estimator” in the rest of the article. It is also sometimes called a “a product limit estimator.”
- [38] M. Greenwood, Reports on Public Health and Medical Subjects, H.M. Stationery Office, 1 (1926).
- [39] D. B. Stouffer, R. D. Malmgren, and L. A. Amaral, “Comment on the origin of bursts and heavy tails in human dynamics,” (2005), arXiv:physics/0510216 [physics.data-an].
- [40] A.-L. Barabási, K.-I. Goh, and A. Vazquez, “Reply to comment on ”the origin of bursts and heavy tails in human dynamics”, ” (2005), arXiv:physics/0511186 [physics.data-an].
- [41] A. Corral, *Phys. Rev. E* **68**, 035102 (2003).
- [42] A. Saichev and D. Sornette, *Phys. Rev. Lett.* **97**, 078501 (2006).
- [43] Ø. Borgan and K. Liestøl, *Scandinavian Journal of Statistics* **17**, 35 (1990).
- [44] National Institute of Standards and Technology, Available at <http://dlmf.nist.gov/>.
- [45] J.-P. Onnela, J. Saramäki, J. Hyvönen, G. Szabó, M. A. de Menezes, K. Kaski, A.-L. Barabási, and J. Kertész, *New J. Phys.* **9**, 179 (2007).

## SUPPLEMENTARY MATERIAL

### Appendix A: Deriving observed inter-event time distributions

In this section, we derive a formula for the probability  $p'(\tau_i, n)$  of observing  $\tau_i$  as the  $i$ th IET in a sequence with exactly  $n$  events. We assume that the sequence is produced by a stationary renewal process with an IET distribution of  $p(\tau)$  and that we observe it in a finite window that starts at time 0 and ends at time  $T$ . We use  $p'(\tau_i, n)$  to approximate  $p'(\tau, n)$  when we observe a large number of independent sequences. See Ref. [9] for an introduction to renewal processes.

The probability that the  $n$ th event after time 0 takes place at time  $t$  is

$$p(t, n) = p_R * p^{*(n-1)}(t), \quad (\text{A1})$$

where  $p_r(\tau_r) = \frac{1}{\mu_1} \int_{\tau_r}^{\infty} p(\tau) d\tau$  is the residual waiting-time distribution,  $*$  is the convolution operator,  $x^{*y}$  means that  $x$  is convolved with itself  $y$  times, and  $\mu_1$  is the expected IET. We use Eq. ((A1)) to calculate the probability  $p'(n)$  of observing exactly  $n$  events during a time window of length  $T$ . The probability  $p'(n)$  is equal to the probability that the  $n$ th event after time 0 takes place at time  $t \leq T$  and the subsequent IET  $\tau_n$  is larger than  $T - t$ . That is, one can write the probability of observing exactly  $n$  events as

$$\begin{aligned} p'(n) &= \int_0^T p(t, n) \int_{T-t}^{\infty} p(\tau) d\tau dt \\ &= \mu_1 p_R * p^{*(n-1)} * p_R(T). \end{aligned} \quad (\text{A2})$$

We now want to calculate the probability of observing  $n$  events when we know the  $i$ th observed IET  $\tau_i$  (where  $i \in \{1, \dots, n-1\}$  and  $n \geq 2$ ). We obtain this probability from Eq. (A2) by substituting  $T$  with  $T - \tau_i$  and  $n$  with  $n - 1$  to yield

$$p'(n|\tau_i) = \mu_1 p_R * p^{*(n-2)} * p_R(T - \tau_i). \quad (\text{A3})$$

The joint probability distribution of observing  $n$  events with  $\tau_i$  as  $i$ th IET is thus

$$p'(n, \tau_i) = p'(n|\tau_i)p(\tau_i). \quad (\text{A4})$$

Observe that the probability distribution (A4) is independent of the index  $i$  as long as  $i \in \{1, \dots, n-1\}$ . However, for a single sequence, the quantities  $\tau_i$  and  $\tau_j$  (with  $i \neq j$ ) are not independent. However, we can use Eq. (A4) to approximate the total distribution of the IETs and the numbers of events as long as there are sufficiently many event sequences.

For a Poisson process, the approximate observed IET distribution given the number of events is

$$p'(\tau|n) = n \frac{(T - \tau)^{n-1}}{T^n}. \quad (\text{A5})$$

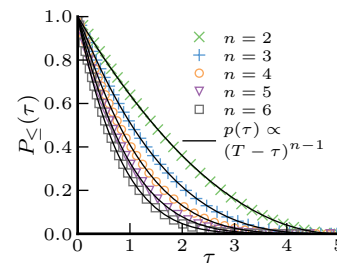


FIG. 4. Cumulative conditional distributions of the IETs given the number of events in a sequence. The simulated data from a stationary Poisson process (markers) corresponds to the theoretical estimates (black solid curves) with an observation-window size of  $T = 5$ . The distributions are independent of the rate of the Poisson process.

The cumulative distribution is thus

$$P'_{\leq}(\tau|n) = \frac{(T - \tau)^n}{T^n}. \quad (\text{A6})$$

Note that Eqs. (A5) and (A6) are independent of the rate of the Poisson process. We illustrate this independence in Fig. 4.

### Appendix B: Kaplan–Meier estimator for inter-event times

We now discuss how to use the Kaplan–Meier (KM) estimator [35] to estimate the IET distribution of a stationary renewal process when one only observes events in a finite time window. Our approach is similar to the “shortcut method” of Denby and Vardi [24]. Unlike them, however, we do not add a point  $\tau_M$  to the IET distribution estimate that is much larger than the observed IET values.

The KM estimator is a nonparametric estimator for lifetimes (or times of death) in the presence of censored lifetimes (or losses) [35]. One observes lifetimes that take place with a total of  $n$  distinct time stamps, where each of the time stamps can correspond either to an observed lifetime  $\tau_i$  or to a censoring time  $\tau_{c,i}$ . (If the lifetime  $\tau_i$  is censored, we say that it is a “censored lifetime,” and we say that the time  $\tau_{c,i}$  that it is censored is its “censoring time.”) For censored lifetimes, we know that the real lifetime is longer than the censoring time:  $\tau_i > \tau_{c,i}$ . The event times are then  $t_i = \tau_i$  if the lifetime is not censored and  $t_i = \tau_{c,i}$  if it is censored, and we order these times so that  $t_1 < \dots < t_{n_d}$ . The KM estimator  $\hat{P}_{\leq}$  for the cumulative distribution of lifetimes is

$$\hat{P}_{\leq}(t) = \prod_{\{i:t_i < t\}} \left(1 - \frac{\delta_i}{n_i}\right), \quad (\text{B1})$$

where  $n_i$  is the number of lifetimes that are at least as long as  $t_i$  or have not been censored at time  $t_i$  (i.e.,  $n_i = \sum_{j \geq i} [\delta_j + c_j]$ ), the parameter  $\delta_i$  is the number of lifetimes

that are observed at time  $t_i$ , and  $c_i$  is the number of lifetimes that are censored at time  $t_i$ .

One can estimate the variance of the KM estimator using Greenwood's formula [35, 38]:

$$\text{Var}(\hat{P}_{\leq}(t)) = \hat{P}_{\leq}^2(t) \sum_{\{i:t_i < t\}} \frac{\delta_i}{n_i(n_i - \delta_i)}. \quad (\text{B2})$$

One can then use the variance estimate to construct confidence intervals for the estimate of an IET distribution. For example if the  $\hat{P}_{\leq}(t)$  values are normally distributed, then the confidence intervals are

$$\hat{P}_{\leq}(t) \pm z_{\alpha/2} \sqrt{\text{Var}(\hat{P}_{\leq}(t))},$$

where  $1 - \alpha$  is the confidence level and  $z_{\alpha}$  is the quantile function of the standard normal distribution. In general, however, the  $\hat{P}_{\leq}(t)$  values are not normally distributed, and this can lead to confidence intervals that are not restricted to lie in the interval  $[0, 1]$ . One usually addresses this situation by applying a transformation  $g$  to the  $\hat{P}_{\leq}(t)$  values to obtain a set of values that better follow a normal-distribution approximation. One can then calculate the confidence interval for the transformed random variable so that

$$g(\hat{P}_{\leq}(t)) \pm z_{\alpha/2} \sqrt{\text{Var}(g(\hat{P}_{\leq}(t)))}.$$

Choices for the transformation include functions  $g(p) = \ln(p)$ ,  $g(p) = \ln(-\ln(p))$ , and  $g(p) = \arcsin(\sqrt{p})$  (see, e.g., Ref. [43] for a discussion about choosing the transformation). In Fig. 3 of the main text, we used the transformation  $g(p) = \ln(p/(1-p))$  to follow the choice in Ref. [24].

One can use the KM estimator to estimate IETs of a renewal process by considering the observed IETs as observed lifetimes and the IETs that are truncated by the end of a time window (i.e., the IETs that are forward censored) as censored lifetimes. If the renewal process is stationary, then one can also repeat this procedure by reversing the direction of time [24]. In other words, one can consider both backward-censoring and forward-censoring times as censored lifetimes, and one counts the observed IETs as observed lifetimes twice. This makes it possible to use the information in the backward-censoring times in the construction of the estimator for the IET distributions. Note that the variance estimator of Greenwood's formula in Eq. (B2) needs to be multiplied by 2 in order to account for the fact that uncensored data points are used twice [24].

### Appendix C: Distributions of number of events

In Fig. 5, we show the distributions for the numbers of events for the empirical data sets of the main text. Most of the people in the data exhibit very little activity, although there are also people that are significantly

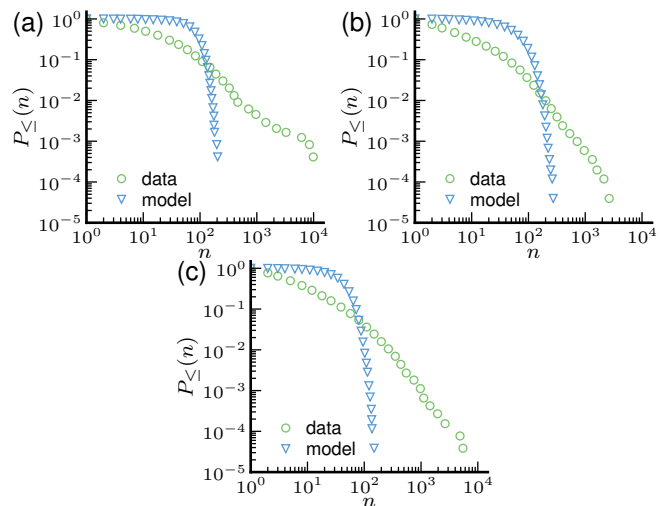


FIG. 5. Cumulative distributions for the numbers of events in several communication data sets. We mark the distribution of the original data using blue crosses, and we use green dots to mark the distribution of the process that assumes that the data were produced by a single IET distribution (see the text for details). (a) Eckmann et al. e-mail data [1], (b) POK messages [4], (c) Wu et al. short message data [7].

more active (by several orders of magnitude). One would not expect such a distribution if all event sequences were produced by a single renewal process. To illustrate this point, we construct a renewal process whose IET distribution we infer using the KM estimator (see Fig. 3). Using this model process, we then produce a new data set that has the same number of event sequences as the original data. We plot the original distribution of IETs and the IET distribution produced by the model processes in Fig. 5. The distributions of events observed in our data sets and the ones observed for the model are significantly different: almost all of the event sequences produced by the renewal process that we construct contain between 10 and 100 events, and there are no sequences with a very small number or a very large number of events. It is clearly not likely that all of the event sequences in the data were produced by a single renewal process.

### Appendix D: Model with a universal characteristic function

The assumption that event sequences are produced by a single IET distribution is very restrictive. One way to relax this assumption is to suppose that each event sequence is produced by an IET distribution with the same characteristic shape  $f$  but with a different mean value  $\tau_0$ . The IET distribution for a model constructed using this assumptions is  $p(\tau|\tau_0) = \frac{1}{\tau_0} f(\tau/\tau_0)$ , where  $\tau_0$  is the mean IET of the sequence. This model has been fitted to several empirical data sets [4, 5, 17, 20, 41, 42].

In Fig. 6, we show numerical results for a model in



which  $f$  is an exponential distribution and we construct the distribution for the mean values  $\tau_0$  so that the numbers of events in the sequences are distributed as a power law. In Fig. 6a, we show both the distribution of observed IETs and a KM estimate when all of the event sequences are grouped together. It is clear that the observed IETs cannot be used to estimate the real IETs, but the KM estimator performs well in this task. One can also group event sequences with similar values for the parameter  $\tau_0$ . Plotting the IET distributions then causes the data to collapse onto a curve that follows the characteristic shape  $f$  if the IET distributions are rescaled with the means of the  $\tau_0$  values. Each group — and especially the groups with large mean values (i.e., with a small number of events) — is of course susceptible to finite-size window effects (see Fig 6b), but one can correct for such effects using the same methods as one would use for data produced by a model with a single IET distribution. See the inset of Fig. 6b.

There is often no way to access the underlying mean IET values. Instead, one has to estimate them from data by calculating the mean IET for each sequence [4, 5, 17, 20]. This introduces another kind of bias, for which the estimators that correct for finite observation windows are not designed. Our example with exponential  $f$  illustrates this situation rather nicely, as one can show (see Section A) that the IET distribution for a sequence that has  $n$  events satisfies  $p(\tau|n, \tau_0) = p(\tau|n) \propto (T - \tau)^{n-1}$ . That is, when grouping event sequences with exactly  $n$  events, we find that (1) their IET distributions are independent of the mean rates  $\tau_0$  and (2) they cannot be rescaled to follow  $f$  even after removing finite-size effects (see Fig. 8 for an illustration).

For each event sequence, we draw an expected IET from the distribution  $p_0(\tau_0)$ . Event sequences are thereby produced by a renewal process with an IET distribution of  $p(\tau) = f(\tau/\tau_0)/\tau_0$ , where  $f$  is the characteristic IET function of the “universal” process. The residual waiting-time distribution [9] for the process is then

$$p_R(\tau_R) = \frac{1}{\tau_0} f_R(\tau_R/\tau_0), \quad (\text{D1})$$

where  $f_R$  is the residual waiting-time distribution for the “universal” process.

Let’s consider a model in which we choose the distributions  $f$  and  $p_0$  so that our model resembles a real-world phenomenon but remains analytically tractable. The distribution for the number of events is often heavy-tailed in communication data [45] (e.g., see Fig. 5), and we choose to model the distribution for the number of events as  $p(n) \propto n^\alpha$  (where  $n \geq 1$ , and  $\alpha = -3$ ). To ensure analytical tractability, we choose the characteristic IET function  $f$  to be an exponential function. That is, our aggregate process is a combination of multiple Poisson processes. By exploiting the relation  $\tau_0 = \frac{T}{n}$ , we can approximate the IET distribution for the aggregate process:

$$p(\tau) \propto \int_1^\infty np(n)p(\tau|n)dn, \quad (\text{D2})$$

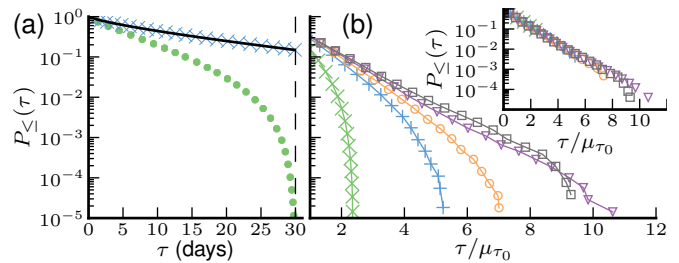


FIG. 6. Numerical calculations for a model in which we produce the event sequences using a universal characteristic shape function  $p(\tau|\tau_0) = \frac{1}{\tau_0} f(\tau/\tau_0)$ , where  $f(\tau) = e^{-\tau}$  and the mean values  $\tau_0$  are distributed such that the expected numbers of events satisfy the probability distribution  $p(n) \propto n^{-3}$  (where  $n \geq 1$ ). (a) Cumulative distribution of observed IETs (green dots) and a KM estimate for the cumulative distribution (blue crosses). The black curve is the theoretical estimate for the real IET distribution  $p(\tau) = E_{\alpha-2}(\tau/T)$ , where  $E_n$  is the exponential integral function [44]. (b) Cumulative distributions of observed IETs when we bin event sequences according to the expected number of observed events  $n = T/\tau_0$  ( $\times$ :  $n \in [2, 3]$ ,  $+$ :  $n \in [5, 6]$ ,  $\circ$ :  $n \in [7, 9]$ ,  $\nabla$ :  $n \in [13, 25]$ ,  $\square$ :  $n \in [50, 150]$ ; we skip every other bin in order to make the figure easier to read). We divide the IETs in each bin by the mean  $\tau_0$  value of the bin  $\mu_{\tau_0}$ . In the inset, we show KM estimates for the cumulative distributions IETs of each bin.

which reduces to

$$p(\tau) = \frac{E_{\alpha-2}(\tau/T)}{TE_{\alpha-1}(1/T)}, \quad (\text{D3})$$

where  $E_\alpha(x) = \int_1^\infty e^{-tx}/t^\alpha dt$  is the exponential integral function [44].

In Fig. 6a, we observed that our KM estimator agrees with the theoretical prediction of Eq. (D3). In Fig. 7, we show similar results to Fig. 6b, except that we show the raw distributions instead of cumulative ones and we apply a correction by applying a linear bias factor instead of using the KM estimator. In Fig. 8, we also show similar results as in Fig. 6b and Fig. 7, except that we calculate our results using the observed number of events instead of using the underlying mean rates to calculate the expected number of events  $n = \frac{T}{\tau_0}$ . The IET distributions of the event sequences with small numbers of events are not correctly identified as exponential distributions, but they follow distribution defined in Eq. (A5) if one uses the observed number of events to group the event sequences.

### Appendix E: Estimating moments and burstiness from individual sequences

It is often undesirable to assume that all event sequences come from the same distribution. For example, in a temporal social network, one might wish to relax this assumption considerably and suppose that each node or edge has an independent renewal process that

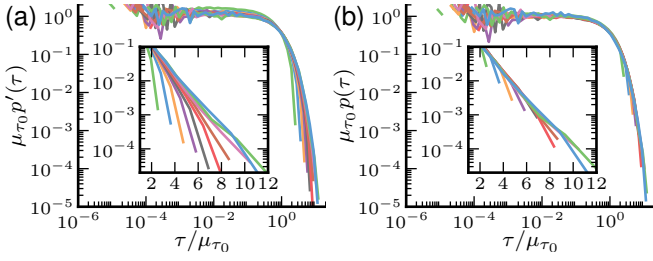


FIG. 7. Numerical calculations for a scenario in which we produce IETs using a model with a universal characteristic shape function D1, where  $f(\tau) = e^{-\tau}$ , and we distribute the mean values so that the expected numbers of events are distributed as  $p(n) \propto n^{-3}$  (where  $n \geq 1$ ). (a) Distributions  $p'(\tau)$  of observed IETs when we bin event sequences according to the expected number of observed events calculated from the mean values  $t_0$ . (b) Distributions  $p(\tau) \propto p'(\tau)/(T - \tau)$  of observed IETs corrected for the linear bias when we bin event sequences according to the expected number of observed events calculated from the mean values  $t_0$ . In both panels, the insets show magnifications of the tails of the IET distributions. Each curve corresponds to a bin with a similar number of expected events  $n = T/\tau_0$ . The bins are  $n \in [2, 3)$ ,  $n \in [4, 5)$ ,  $n \in [5, 6)$ ,  $n \in [7, 9)$ ,  $n \in [9, 13)$ ,  $n \in [13, 25)$ ,  $n \in [25, 50)$ , and  $n \in [50, 150)$ .

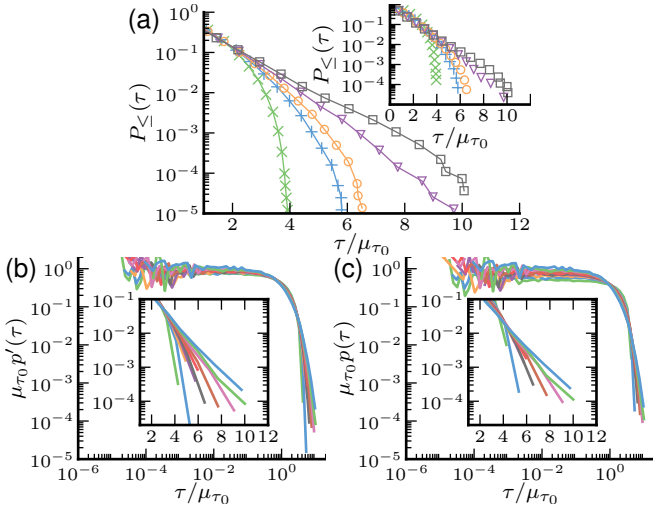


FIG. 8. Numerical calculations for a scenario in which we produce IETs using a model with a universal characteristic shape function D1, where  $f(\tau) = e^{-\tau}$ , and we distribute the mean values so that the expected numbers of events are distributed as  $p(n) \propto n^{-3}$  (where  $n \geq 1$ ). We bin each of the sequences according to the observed number of events  $n$ . (a) Cumulative distributions of observed IETs when we bin event sequences according to the expected number of observed events  $n = T/\tau_0$ . (Inset) The KM estimate for cumulative distributions IETs ( $\times$ :  $n \in [2, 3)$ ,  $+$ :  $n \in [5, 6)$ ,  $\circ$ :  $n \in [7, 9)$ ,  $\nabla$ :  $n \in [13, 25)$ ,  $\square$ :  $n \in [50, 150)$ ; we skip every other bin in order to make the figure easier to read). (b) Distributions of observed IETs. (c) Distributions of observed IETs corrected for the linear bias. The insets in the bottom panels show magnifications of the tails of the IET distributions.

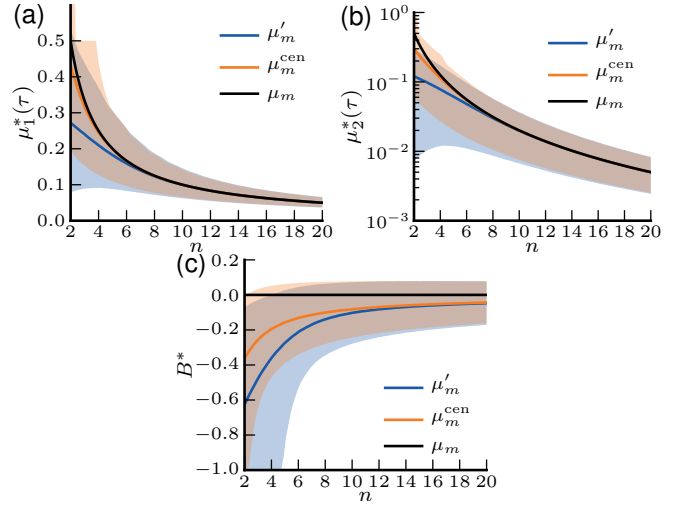


FIG. 9. Estimates for the (a) first and (b) second moment and (c) the burstiness for single-event sequence produced with a stationary Poisson process with a rate  $n/T$ , where  $n$  is the expected number of events and  $T$  is the size of the observation window. The solid curves give the mean estimator value as a function of the expected number of events. The shaded region corresponds to the values inside of the 10% and 90% percentiles. The black curves are the real values for the moments and the burstiness for the process.

produces the events that are associated to it. In this case, the number of IET distributions can be very large, and it is therefore desirable to calculate summary statistics for those distributions instead of considering the full distributions. We illustrate this idea using the first two moments of IET distributions,  $\mu_1(\tau)$  and  $\mu_2(\tau)$ , which can be used to calculate variance, a “burstiness” measure  $B = \frac{\sqrt{\mu_2(\tau) - \mu_1(\tau)}}{\sqrt{\mu_2(\tau) + \mu_1(\tau)}}$  [20], and the mean residual waiting time. All three of these quantities give useful diagnostics to aid in the understanding of simple spreading processes such as the SI model or the SIR model [15–18]. Burstiness has also been used to classify different types of event-generating processes [20].

There are two important issues when calculating moments of an IET distribution: (1) the length bias in the observed IETs; and (2) lack of information about the IET distribution for times  $\tau > T$ , where  $T$  is the size of the time window. Ignoring these problems and using the uncorrected IET distributions to calculate the moments yield lower bounds for them, because

$$\begin{aligned} \int_0^T \tau^m p'(\tau) d\tau &\leq \int_0^T \tau^m p(\tau) d\tau \\ &\leq \int_0^T \tau^m p(\tau) d\tau + T^m P_{\leq}(T) \\ &\leq \int_0^{\infty} \tau^m p(\tau) d\tau. \end{aligned} \quad (\text{E1})$$

As we demonstrated in Fig. 2 of the main text, the KM estimator can give very good estimates for the IET

distribution if we group together a large number of event sequences. However, for individual sequences, the KM estimator is not necessarily the best choice. For example, if the censored IETs are larger than the observed IETs, then the KM estimator ignores the censored times and gives the exact observed IET distribution. For a single event sequence with  $n$  IETs  $\tau_i$ , we can write the estimator of the  $m$ th moment for the observed IETs as  $\mu'_m = \frac{\sum_i \tau_i^m}{n}$ . We can take a similar approach as in Eq. (3) and also include the censored IETs to get a slightly better estimate of the  $m$ th moment (see Fig. 9). This yields

$$\mu_m^{\text{cen}} = \frac{\tau_{cf}^m + \tau_{cb}^m + 2 \sum_i \tau_i^m}{2(n+1)}. \quad (\text{E2})$$

Both  $\mu'_m$  and  $\mu_m^{\text{cen}}$  will be biased towards underestimating the moments of the real IET distributions if they are used to estimate the moments of the real IET distributions. However,  $\mu_m^{\text{cen}}$  is likely to produce better estimates than  $\mu'_m$ . See Fig 9, where we show how the estimators behave if the data are produced by a stationary Poisson process. The errors that the two estimates produce are likely to be higher if the IET distribution has a heavier tail than that of the IET distribution of a Poisson process. However, these results illustrate an important point: if the event sequences have only a few events, then using the observed IETs to calculate the moments will signif-

icantly underestimate the moments even if the data are produced by a stationary Poisson process.

The length bias can have a significant effect on the moments of an event sequence and on related values such as burstiness and residual waiting times. Consider a situation in which one needs to calculate moments or burstiness for single-event sequences with a small number of events. In such cases, assuming that one does not possess a priori information about the distribution, one should at least estimate the bias in the results under the assumption that similar data would have been produced by a Poisson process. In this situation, one can use the results of Fig. 9 to provide a rough guideline: if the sequence has fewer than 6 events, then even the mean IET has a substantial bias. For the second moment, one needs a few more events to be accurate, and the burstiness values (which, as discussed above, have been used to give insights into human dynamics in communication processes) can be biased even for event sequences with many dozens of events. The bias is always towards making the values lower.

#### Appendix F: An additional illustration of IET distributions of empirical data

Figure 10 corresponds to Fig. 3 in the main text, but we now plot the IET distributions using doubly logarithmic axes.

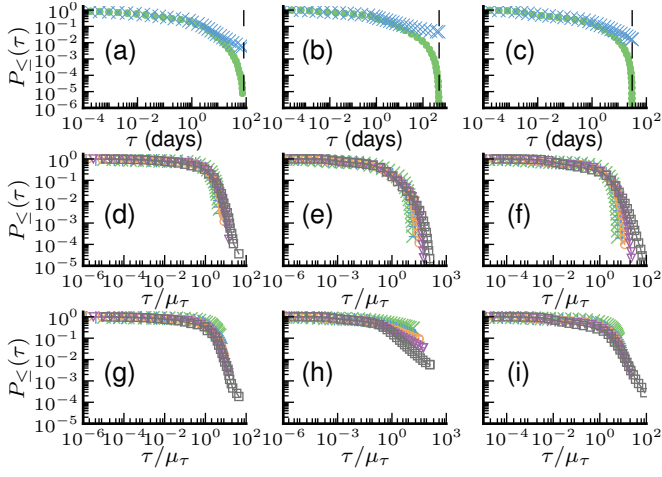


FIG. 10. Results for the empirical data sets plotted using doubly logarithmic axes. Panels (a)–(c) show IET distributions for all node activation sequences. The dots mark the observed IET distributions, and the crosses mark the estimates of the original IET distributions using the KM estimator. Panels (d)–(f) show cumulative distributions of observed IETs, and panels (g)–(i) show KM estimates for the cumulative IET distributions. We bin the event sequences according to the number of events in them ( $\times$ :  $n = 2$ ,  $+$ :  $n = 5$ ,  $\circ$ :  $n \in [7, 8]$ ,  $\nabla$ :  $n \in [13, 24]$ ,  $\square$ :  $n \in [50, 149]$ ; we skip every other bin in order to make the figure easier to read), and we normalize them according to the bin’s mean IET  $\mu_{\tau}$ . The data sets are (a, d, g) Eckmann et al. e-mail data [1], (b, e, h) POK messages [4], and (c, f, i) Wu et al. short message data [7].